Arch. Min. Sci. **70** (2025), 3, 387-402

Electronic version (in color) of this paper is available: http://mining.archives.pl

DOI: https://doi.org/10.24425/ams.2025.156291

ZHIHENG CHEN[1], JUNHUA XUE[1], JIAN XIAO[1],
RENHUI CHENG[1], TONGSHUANG LIU[1*]

RESEARCH ON DEPRESSURIZATION GAS EXTRACTION TECHNIQUES AND IDENTIFICATION OF GAS SOURCESI GOAF BASED ON CARBON AND HYDROGEN ISOTOPE TRACING

In the mining environment of coal seams, in order to accurately quantify the gas sources in the goaf of the protective layer working face and effectively implement gas extraction and control, this paper conducts experiments on gas source identification in the goaf in the Pingdingshan mining area. By collecting desorbed gas samples from the parent coal seam, a detailed analysis of the gas components (including methane, ethane, carbon dioxide) as well as the values and distribution characteristics of stable carbon and hydrogen isotopes was conducted. Based on these data, we established a calculation model for gas source identification in the goaf based on stable carbon and hydrogen isotopes and component averages, achieving a quantitative calculation of gas sources from various coal seams as the goaf advances, and implementing depressurization gas extraction techniques for coal seams at a greater distance upward. The results show significant differences in the stable carbon and hydrogen isotopes of desorbed gases from the three coal seams, although the overall trend is relatively consistent. As the burial depth of the coal seam increases, the carbon isotope values of methane, ethane, and carbon dioxide, as well as the hydrogen isotope values of methane, all show a trend of becoming heavier. In addition, the main source of gas in the goaf of the protective layer comes from the downward adjacent coal seam, accounting for 81% of the total source, while the average contribution from the same coal seam is 12%, and the contribution from distant upward coal seams is 7%. By implementing depressurization gas extraction techniques for distant upward coal seams, we also identified the optimal window period for depressurization extraction in the C_1 coal seam to be between 85 and 100 days.

Keywords: Protective layer; Goaf; Carbon and hydrogen isotopes; Gas source; Time window period

[1] XI'AN UNIVERSITY OF SCIENCE AND TECHNOLOGY, CHINA

* Corresponding author: Liutongshuang79@126.com

1. Introduction

Deep mining of coal resources has become a trend, but deep mining is facing serious threats such as gas disasters, rockburst disasters, and mine floods [1-4]. Moreover, there are many high gas mines in deep China, and the complexity of the deep environment further increases the difficulty of preventing and controlling gas disasters, posing a threat to the safety production of coal mines. Meanwhile, the occurrence forms of deep coal seam clusters are quite common. Therefore, conducting precise identification and proportion determination of gas sources in the goaf of protective layer mines has important technical and theoretical significance for improving the efficiency of mine depressurization gas extraction, and optimizing process design and parameter settings.

Gas prevention and control in the goaf is a key measure to control the gas concentration exceeding limits at the working face [5]. Domestic and international studies show that the main sources of gas include coal walls, fallen coal, residual gas in the goaf, and gas from adjacent layers [6-9]. In the research on the analysis of gas sources in the goaf, scholars often use methods such as theoretical analysis [10], physical simulation [11], and numerical simulation [12] to study the flow rules and concentration distribution of gas, further determining the sources of gas. In particular, using CFD software to establish a gas permeation model and conducting numerical analysis through software such as Fluent to simulate and study the movement of gas in the mining area [13-18], thereby grasping the changing rules of gas concentration.

Traditional methods for identifying gas sources in the goaf, such as statistical analysis [19], neural networks [20], and grey systems [21], although showing advantages in applicability, accuracy, and system integrity, still have room for improvement in enhancing accuracy and conducting multilayer joint analysis. Stable carbon isotope technology shows unique advantages in studying the carbon cycle, source tracing, and migration trajectory monitoring in nature [22]. By analyzing the gas composition and carbon isotope values in gas samples from the goaf, the components and sources of gas can be effectively determined, becoming an important means for quantitative analysis of gas sources in the goaf [23-25].

This study selects a mine in Pingdingshan City, Henan Province, as the research object. During the mining period of the C_2 protective layer, carbon and hydrogen isotope tracing technology is used to study the gas sources and their proportions in the C_2 goaf. Based on this, precise gas extraction is carried out for the distant upward C_1 coal seam, and the optimal time window period for gas extraction in the C_1 coal seam during the mining period of the C_2 coal seam is studied. This research provides valuable references for gas control work in Pingdingshan and other similar mining areas.

2. Project overview and sampling test

2.1. Project background introduction

The coal mine targeted in this study is located in Pingdingshan City, Henan Province, and is a mine prone to outbursts. The main coal seams include C_1, C_2, and C_3. The positional relationship of these three coal seams is shown in Fig. 1. The average thickness of the C_1 coal seam is 2.2 meters, with its pseudo-roof consisting of mudstone or carbonaceous mudstone, its direct

roof composed of mudstone, sandy mudstone, or sandstone, and its old roof being medium-coarse sandstone. The floor is made up of mudstone or sandy mudstone. In areas close to geological structures, joints and fractures are relatively developed, usually aligned with the direction of geological structures.

The C_2 coal seam, being the protective layer mined in this study, has an average thickness of 2 meters. Its direct roof is blocky gray and dark gray mudstone, with the old roof being gray-white or light gray fine to medium quartz sandstone; its direct floor is also gray and dark gray mudstone, with the bottom being sandy mudstone, and the old floor being gray and dark gray medium sandstone.

The average thickness of the C_3 coal seam is 1.6 meters, with its direct roof made of medium sandstone or sandy mudstone, both the upper roof and pseudo-roof being sandy mudstone, and the floor also consisting of sandy mudstone. The average interlayer distance between the C_2 coal seam and the C_1 coal seam is 75 meters, while the distance between the C_2 and C_3 coal seams is 10 meters, the average burial depth of C_2 coal seam is 940 m.

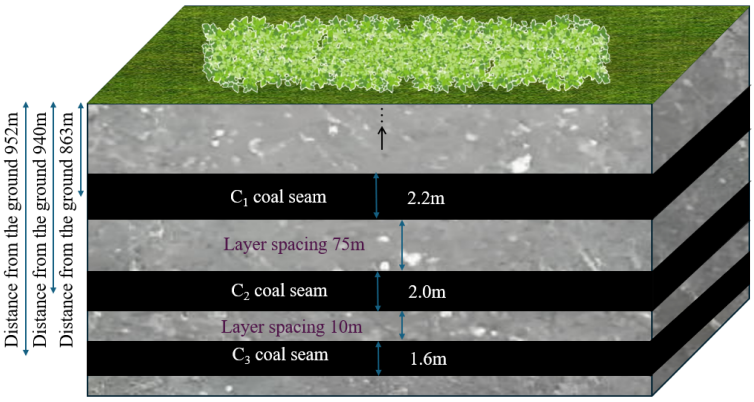

Fig. 1. Schematic diagram of the main mining coal seams

2.2. Sampling and testing

Coal samples from the main mining coal seams C_1, C_2, and C_3 were collected as parent samples, with three coal samples collected from each layer. According to the testing requirements, the collection area must be within the range of the C_2 working face. After sampling, the coal samples should be immediately placed into sampling cans, completely filled into the cans and compacted, and quickly sealed, then sent to the surface laboratory. To ensure the uniformity and representativeness of the data, five sets of desorbed gas samples were extracted from the coal samples taken for analysis of gas components and stable carbon and hydrogen isotopes. The testing work mainly includes two parts: gas component testing and stable carbon and hydrogen isotope testing. The analytical gas sample component testing instrument is the GC-7800 gas chromatograph, the stable carbon and hydrogen isotope testing instrument for methane, ethane, and carbon dioxide in the analytical gas samples is the DELTA plus stable isotope mass spectrometer, and the stable hydrogen isotope testing instrument for methane is the gas chromatography-isotope ratio mass spectrometer (GC/TC/Delta Plus XL).

3. Analysis of stable hydrocarbon isotope gas test results

3.1. Principle of stable carbon and hydrogen isotope tracing technology

^{13}C and ^{12}C are two stable carbon isotopes with significant tracing implications. However, the natural abundance of ^{12}C is much greater than that of ^{13}C, making it difficult to represent its isotopic composition by absolute abundance [26]. Therefore, its isotopic composition is usually represented by a relative quantity, also known as the isotopic ratio δ (abundance ratio of $^{13}C/^{12}C$), which is defined as:

$$\delta^{13}C(‰) = [\frac{(^{13}C / {}^{12}C)_S}{(^{13}C / {}^{12}C)_{PDB}} - 1] \times 1000 \quad (1)$$

In the formula, $(^{13}C/^{12}C)$ s is the abundance ratio of ^{13}C and ^{12}C in the actual measured sample; $(^{13}C/^{12}C)$ PDB is the internationally recognized abundance ratio of ^{13}C and ^{12}C in the PDB standard sample. Since ^{13}C is very small, carbon isotope values are usually expressed in permille.

Due to the age and formation environment of the strata being different (dynamic fractionation and equilibrium fractionation), fractionation effects of carbon and hydrogen isotopes occur, leading to significant differences in carbon and hydrogen isotopes between different strata. Therefore, by analyzing the carbon and hydrogen isotope values in the actual samples and combining them with isotope distribution maps, one can infer the source layer [27-28].

3.2. Stable carbon and hydrogen isotope distribution characteristics in coal seam desorbed gas

3.2.1. Desorption gas composition and stable hydrocarbon isotope master test

During the experimental phase, 15 sets of desorbed gas were extracted from the 9 coal samples collected from the 3 coal seams, and analyses of gas components and stable carbon and hydrogen isotopes were conducted. The main testing indicators for the gas components are N_2, CO_2, CH_4, and C_2H_6. The average values of the gas component and related isotope test results are shown in the following table.

TABLE 1

Statistical table of parent component and isotope characteristics

Coal seam	Gas composition				Carbon isotope value			Hydrogen isotope value
	CH_4	C_2H_6	N_2	CO_2	$\delta\,^{13}CCH_4$	$\delta\,^{13}CC_2H_6$	$\delta\,^{13}CCO_2$	$\delta\,HCH_4$
	Average %	Average %	Average %	Average %	Average ‰	Average ‰	Average ‰	Average ‰
C_1	79.98	0.0028	10.12	9.902	–40.32	–19.05	–22.89	–182.448
C_2	80.16	0.0031	9.56	10.278	–38.46	–18.12	–20.53	–178.125
C_3	80.56	0.0035	8.92	10.517	–37.22	–16.82	–17.99	–172.61

3.2.2. Analysis of desorption gas composition and stable hydrocarbon |isotope results

Five sets of desorbed gas samples from each main mining coal seam were tested for gas components and their related isotope values. The results of the gas component tests for each coal seam are shown in Fig. 2.

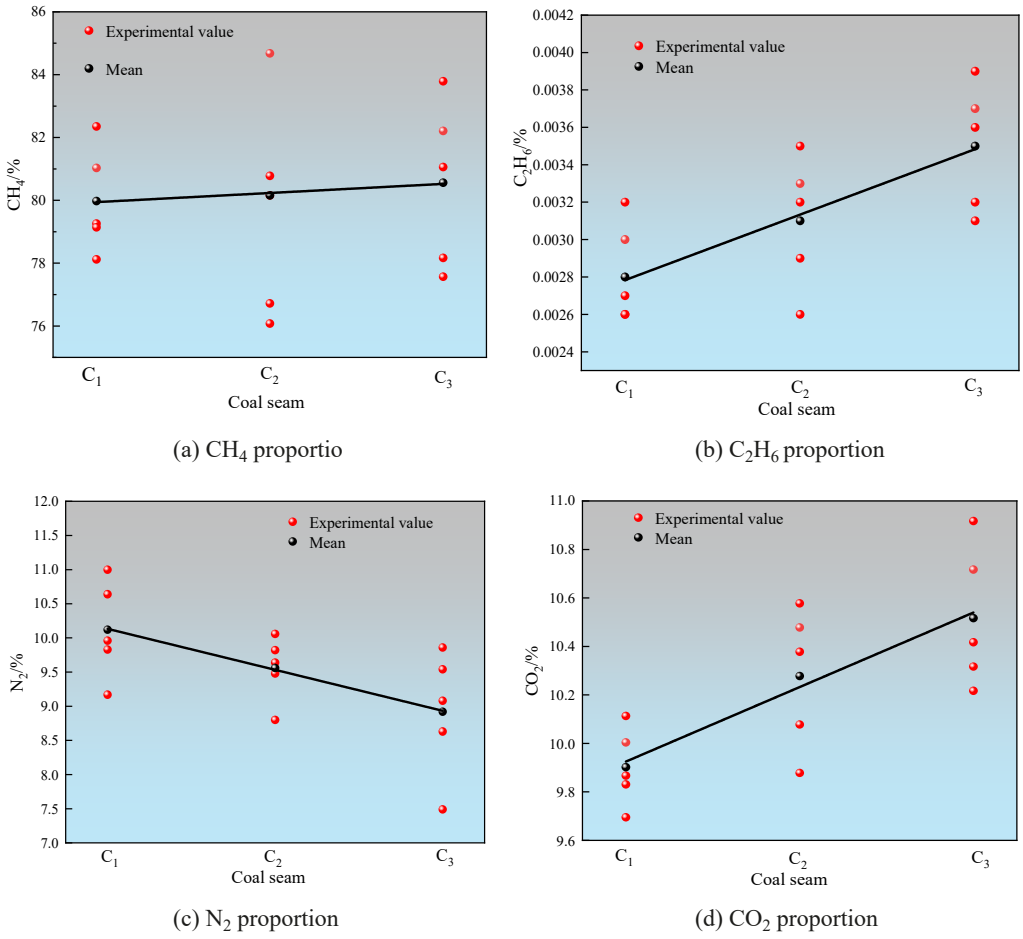

(a) CH_4 proportio (b) C_2H_6 proportion

(c) N_2 proportion (d) CO_2 proportion

Fig. 2. Distribution characteristics of desorbed gas components in each coal seam

From Fig. 2, it can be seen that there are some differences in the composition of desorbed gas among the three coal seams. The measured proportion of methane (CH_4) ranges from 76.08% to 84.68%. Specifically, the methane content in the C_1 coal seam ranges from 78.12% to 82.35%, in the C_2 coal seam from 76.08% to 84.68%, and in the C_3 coal seam from 77.57% to 83.39%. The maximum and minimum average differences in methane content across the three seams are 0.58%, indicating small variations.

The measured proportion of ethane (C_2H_6) is between 0.002% and 0.004%, showing that the variation in this gas is relatively small across the three coal seams and the proportion is very low. The measured proportion of nitrogen (N_2) ranges from 7.49% to 11%, with the N_2 content in the C_1 coal seam ranging from 9.17% to 11%, in the C_2 coal seam from 8.8% to 10.06%, and in the C_3 coal seam from 7.49% to 9.86%. The maximum and minimum average differences in nitrogen content across the seams are 1.2%, showing small variations.

The measured proportion of carbon dioxide (CO_2) ranges from 9.695% to 10.917%, with the CO_2 content in the C_1 coal seam ranging from 9.695% to 10.113%, in the C_2 coal seam from 9.878% to 10.582%, and in the C_3 coal seam from 10.217% to 10.935%. The maximum and minimum average differences in CO_2 content across the seams are 0.615%, indicating small variations.

Overall, the analysis shows that the proportions of methane, ethane, and carbon dioxide in the desorbed gas from the three coal seams show a slight increasing trend with increasing burial depth of the coal seam, while the proportion of nitrogen shows a slight decreasing trend. The overall distribution characteristics of the four gas components are methane > carbon dioxide > nitrogen > ethane.

During the experimental process, stability tests were conducted on methane carbon isotopes, ethane carbon isotopes, carbon dioxide carbon isotopes, and methane hydrogen isotopes. To gain a detailed understanding of the distribution patterns and characteristics of stable carbon and hydrogen isotopes in the desorbed gas from the three coal seams, distribution maps of carbon isotope values and hydrogen isotope values for desorbed gas from different coal seams were drawn, as shown in Figs. 3 to 6.

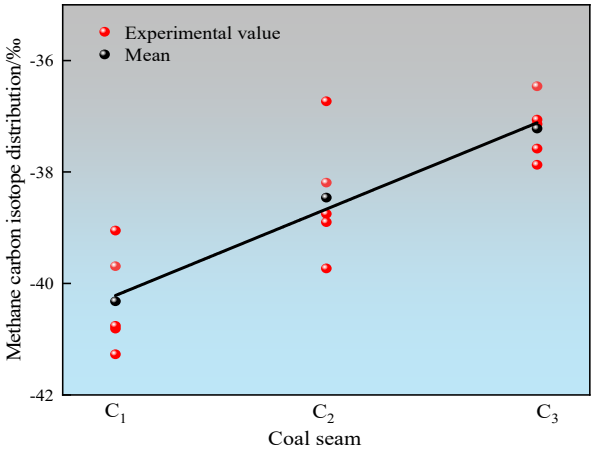

Fig. 3. Methane carbon isotope distribution characteristics

According to the data in Fig. 3, it can be observed that as the depth of the strata increases, the methane carbon isotope values in the desorbed gas from each coal seam gradually become heavier (the absolute values decrease), with the average values fluctuating slightly, mainly concentrated between –40.81 to –36.73‰. This change is mainly due to the increase in burial depth of the coal seams, which corresponds to an increase in the methane content in the desorbed gas. Although the methane carbon isotope values between different coal seams show some differences,

the distribution of their average values does not show significant fluctuations, indicating that the variation trend of methane carbon isotopes in each coal seam is relatively stable. This reflects the consistency of the coal-forming environment and the stability of the fractionation effect.

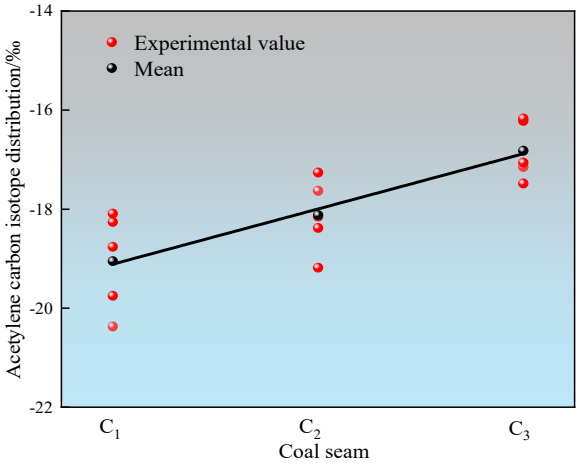

Fig. 4. Ethane Carbon Isotope Distribution Characteristics

From Fig. 4, it is evident that the overall trend in the distribution of ethane carbon isotopes across the coal seams is consistent with that of methane carbon isotopes; that is, they become heavier (the absolute values decrease) with increasing mining depth of the coal seams. The content of ethane gas components in the desorbed gas from each coal seam is extremely low, and the fluctuations in the distribution of ethane carbon isotopes in the desorbed gas from the coal seams are not significant. The average values are generally maintained between –19.05 to –16.82‰.

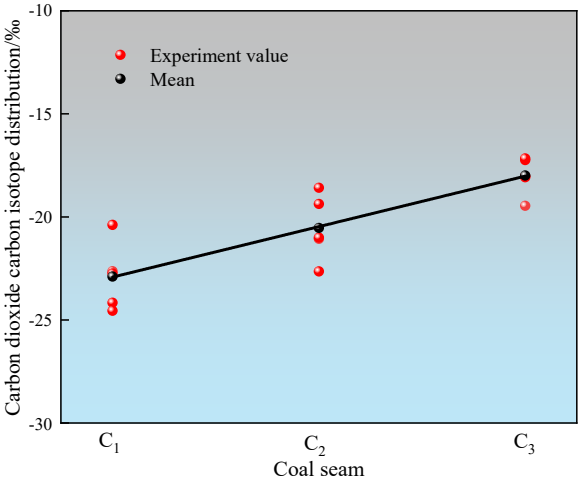

Fig. 5. Carbon dioxide carbon isotope distribution characteristics

From the distribution characteristics of carbon dioxide carbon isotope values in the three coal seams shown in Fig. 5, it can be seen that the variation trend of carbon dioxide carbon isotopes in the desorbed gas from each coal seam is similar to that of methane and ethane carbon isotopes. They also maintain a trend of becoming heavier (the absolute values decrease) with increasing burial depth of the coal seams. The fluctuation range of the average carbon dioxide carbon isotope values across the three coal seams is between –22.89 to –17.99‰, indicating that the differences in carbon dioxide carbon isotopes among the coal seams are relatively small.

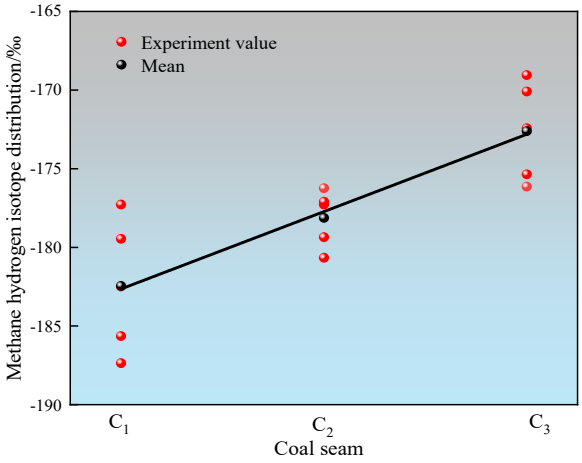

Fig. 6. Methane hydrogen isotope distribution characteristics

According to the data presented in Fig. 6, as the depth of the coal seams increases, the measured values of methane hydrogen isotopes in each coal seam generally show a trend of becoming heavier, and this trend is more significant compared to the other three types of isotopic indicators, with a larger fluctuation range, mainly concentrated between –187.36 to –169.05‰. This phenomenon is mainly due to the significant increase in hydrogen content with the increasing burial depth of the coal seams, accompanied by an acceleration of the fractionation effect.

A comprehensive analysis indicates that the stable carbon and hydrogen isotopes in the desorbed gas from the three coal seams in this mining area exhibit certain differences, but the overall change trend is relatively consistent. As the burial depth of the coal seams increases, the values of methane carbon isotopes, ethane carbon isotopes, carbon dioxide carbon isotopes, and methane hydrogen isotopes all show a trend of becoming heavier. This reflects that the content of methane, ethane, and carbon dioxide in the coal seams increases with the increase in burial depth. The measured isotope values of each coal seam are not affected by hydrodynamic activities or tectonic cutting phenomena, and they accurately reflect the relationship between the changes in burial depth of coal-bearing strata, gas content, and measured isotope values, revealing the distribution characteristics of stable carbon and hydrogen isotopes. This provides an important foundation for subsequent quantitative analysis and identification of the proportion of mixed gas emissions in the goaf of the C_2 protective layer.

3.2.3. Based on the source calculation model for stable carbon and hydrogen isotope tracing analysis

When the source of mixed gas in the goaf of the protective layer comes from multiple coal layers, the calculation formula for stable isotopes in one component of the mixed gas [29,30] is as follows:

$$\delta mix = \frac{V_A \cdot \delta_A + V_B \cdot \delta_B + V_C \cdot \delta_C + \cdots V_N \cdot \delta_N}{V_A + V_B + V_C + ... + V_N} \tag{1}$$

The gas mixture per unit volume has the following relationship:

$$V_N = n \cdot X_n \tag{2}$$

Substituting formula (2) into formula (1) yields:

$$\delta mix = \frac{a \cdot X_A \cdot \delta_A + b \cdot X_B \cdot \delta_B + c \cdot X_C \cdot \delta_C + \cdots n \cdot X_N \cdot \delta_N}{a \cdot X_A + b \cdot X_B + c \cdot X_C + ... + n \cdot X_N} \tag{3}$$

$$\text{Among } a + b + c + ... + n = 1 \tag{4}$$

In the formula, δmix represents the isotopic value of a single component gas measured in the mixed gas; X represents the content of a component gas in the desorbed gas from each coal seam; δ_n represents the isotopic value of a component gas in the desorbed gas from each coal seam.

Since the number of main coal seams measured is three, the resulting source apportionment calculation model is as follows:

$$\begin{cases} \delta mix = \dfrac{a \cdot X_{C1} \cdot \delta_{C1} + b \cdot X_{C2} \cdot \delta_{C2} + c \cdot X_{C3} \cdot \delta_{C3}}{a \cdot X_{C1} + b \cdot X_{C2} + c \cdot X_{C3}} \\ a + b + c = 1 \end{cases} \tag{5}$$

In the formula, a, b, c represent the proportions of gas from each coal seam in the mixed gas; X_{Ci} represents the content of one component gas in the desorbed gas from one of the three measured coal seams; δ_{Ci} is the isotopic value of that component gas. According to Fig. 2(b), the proportion of ethane in the three coal seams is extremely small, ranging between 0.002% and 0.004%, hence this component index is discarded, along with the ethane carbon isotope index. Ultimately, methane carbon isotopes, carbon dioxide carbon isotopes, methane hydrogen isotopes, and related gas components are used as calculation indices, and are combined with the equation to solve for the proportion of gas sources from each coal seam in the mixed gas.

3.3. Identification of gas sources in the goaf

The sampling locations for mixed gas from the C_2 coal seam are located in the goaf 200 meters, 240 meters, and 300 meters behind the working face, with 5 sets of mixed gas samples taken at each sampling location. Experimental tests are conducted on the collected mixed gas samples from the goaf, resulting in 15 sets of mixed gas samples with gas composition and carbon-hydrogen isotope values. The test results are shown in TABLE 2.

TABLE 2

Test Values of mixed gas sample components from the goaf of the c_2 working face

Sampling spot	Gas component (%)				Carbon isotope value (‰)			Hydrogen isotope value (‰)
	CH_4	C_2H_6	CO_2	N_2	$\delta\ ^{13}CCH_4$	$\delta\ ^{13}CC_2H_6$	$\delta\ ^{13}CCO_2$	$\delta\ HCH_4$
The goaf is 200 m away from the working face	73.58	0.003	16.58	9.837	–41.49	–20.05	–11.29	–192.37
	74.63	0.002	17.38	7.988	–40.91	–30.07	–10.77	–189.67
	73.65	0.002	16.59	9.758	–41.45	–30.07	–11.28	–192.19
	74.36	0.001	17.31	8.329	–41.08	–60.04	–10.86	–190.44
	74.64	0.002	17.28	8.078	–40.89	–30.23	–10.82	–189.58
The goaf is 240 m away from the working face	76.57	0.003	16.54	6.887	–39.83	–20.36	–11.28	–184.67
	76.37	0.003	17.82	5.807	–39.99	–20.29	–10.56	–185.32
	75.46	0.002	18.54	5.998	–40.41	–30.54	–10.06	–187.39
	76.38	0.003	17.36	6.257	–39.95	–20.33	–10.79	–185.21
	76.68	0.002	19.27	4.048	–39.78	–30.65	–9.71	–184.43
The goaf is 300 m away from the working face	78.35	0.003	18.46	3.187	–38.96	–20.40	–10.18	–180.58
	77.87	0.004	18.26	3.866	–39.15	–15.35	–10.21	–181.53
	78.12	0.003	17.16	4.717	–39.04	–20.53	–10.90	–180.97
	77.94	0.004	17.89	4.166	–39.14	–15.32	–10.46	–181.45
	78.22	0.003	17.30	4.477	–39.00	–20.43	–10.82	–180.80

By analyzing the test results of the mixed gas from the goaf in conjunction with the test values of the parent coal seam from TABLE 1, and using Equation (5) for calculation, we can determine the source composition of the mixed gas samples in the C_2 goaf and the proportions of each component gas. This is shown in TABLE 3 below.

TABLE 3

Proportions of mixed gas sources in the goaf

Sampling spot	C_1 coal seam	C_2 coal seam	C_3 coal seam
The goaf is 200m away from the working face	0.06	0.12	0.82
	0.05	0.12	0.83
	0.06	0.13	0.81
	0.05	0.11	0.84
	0.06	0.13	0.81
The goaf is 240m away from the working face	0.06	0.10	0.89
	0.07	0.11	0.82
	0.06	0.13	0.81
	0.08	0.13	0.79
	0.07	0.12	0.81
The goaf is 300m away from the working face	0.10	0.12	0.78
	0.08	0.14	0.78
	0.09	0.11	0.80
	0.07	0.12	0.81
	0.11	0.12	0.77

TABLE 3 shows the proportion of mixed gas sources at different mining distances in the goaf. It can be seen from the table that the average source of mixed gas at different distances in the goaf of C_2 coal seam is 0.82, 0.81 and 0.79, respectively. The average value of C_2 coal seam is 0.12, while the average value of C_1 coal seam is 0.06, 0.07 and 0.09, respectively. Among them, C_3 coal seam has a slightly decreasing trend with the mining distance, while C_1 coal seam has a slightly increasing trend on the contrary. This also shows that the gas source of the influx into the C_2 coal seam is mainly the lower adjacent C_3 coal seam, which is the lowest in this coal layer, and the contribution proportion of the C_1 coal seam is the least. This is because the C_2 coal seam has a pressure relief effect on the upper and lower protected layers after mining, while the C_3 coal seam has a large amount of fissure gas flowing into the C_2 coal seam, the C_1 coal seam fissure is not fully developed, and a small amount of gas is sucked into the C_2 coal seam. To avoid the impact of sampling locations on the test results, we conducted further analysis on the gas proportions from different sources at three sampling points within the coal seam. The distribution of gas sources at these three sampling points is shown in Fig. 7.

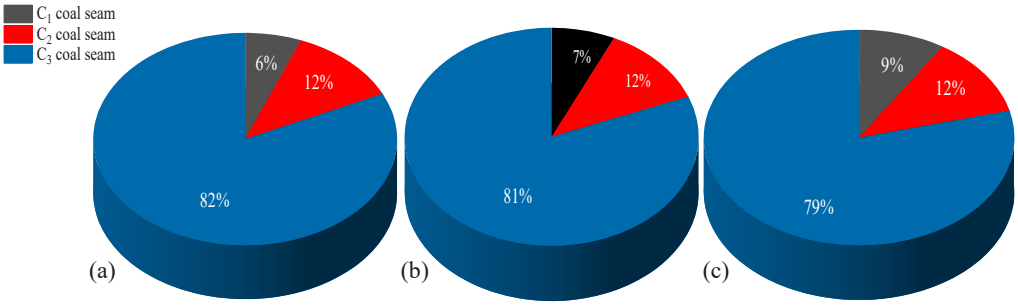

Fig. 7. Gas source proportions at different sampling locations in the goaf
(a) The goaf is 200 m away from the working face, (b) The goaf is 240 m away from the working fac,
(c) The goaf is 300 m away from the working face

As shown in Fig. 7, the gas primarily originates from the C_3 coal seam at different sampling locations. In the mixed gas samples collected 200 meters, 240 meters, and 300 meters behind the working face, the proportion of gas from the C_3 coal seam is 82%, 81%, and 79% respectively; while the proportion from the C_2 coal seam is stable at 12%; Finally, the average proportion of C_1 coal seam is 6%, 7% and 9% respectively. This indicates that during the mining of the protective layer C_2 coal seam, due to the close proximity of the C_3 coal seam to the C_2 coal seam, a near-distance protective layer mining relationship is formed, with the C_3 coal seam located in the floor fracture zone, where a large amount of depressurized gas is introduced into the protective layer above. Meanwhile, the C_1 coal seam, located in the bending subsidence zone of the overlying rock in the goaf, lacks sufficient vertical fractures, hence the gas hazard from the C_1 coal seam still exists. Therefore, when mining the C_2 coal seam (protective layer), targeted measures should be taken to handle the gas from the distant C_1 coal seam above, to eliminate gas hazards and ensure the safe recovery of the protective layer working face.

4. Engineering practice of pressure relief gas drainage in long distance protected coal seam (C_1 Coal Seam)

4.1. Introduction to engineering practice

In the outer misaligned machine roadway high-extraction roadway and the inner misaligned airway high-extraction roadway of the C_2 coal seam working face, cross-layer depressurization gas extraction boreholes aimed at the C_1 coal seam were implemented. These boreholes are arranged in groups every 20 meters, with each group consisting of 3 boreholes, laid out along the inclination direction of the working face. Specifically, the final hole position of the 1# cross-layer borehole is located 15 meters outside the boundary line of the protected range of the C_1 protected layer working face; the final hole position of the 2# cross-layer borehole is located 30 meters inside the boundary line of the protected range of the C_1 protected layer working face; the final hole position of the 3# cross-layer borehole is located 50 meters outside the boundary line of the protected range of the C_1 protected layer working face. The plan and sectional views are respectively shown in Figs. 8 and 9.

In the outer misaligned machine roadway high-extraction roadway, a total of 68 groups of cross-layer boreholes are arranged along the direction of the working face, using a full negative pressure networked extraction method. In the inner misaligned airway high-extraction roadway, due to the proximity of the roadway to the working face and the greater impact of mining, resulting in poorer roadway stability, a total of 30 groups of cross-layer boreholes are arranged here, using a closed naked extraction method.

Through the cross-layer boreholes constructed in the airways and machine roadways high-extraction roadways, along with the mining depressurization impact of the lower protective layer C_2 coal seam on the upward distant protected layer C_1 coal seam, the gas from the protected layer C_1 coal seam is safely and efficiently depressurized and extracted during the mining process of the lower protective layer.

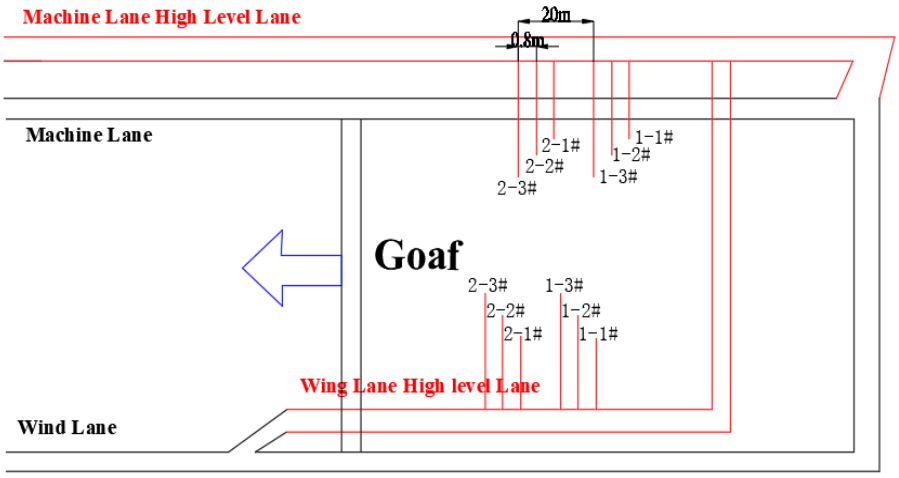

Fig. 8. Layout plan of cross layer pressure relief pumping boreholes

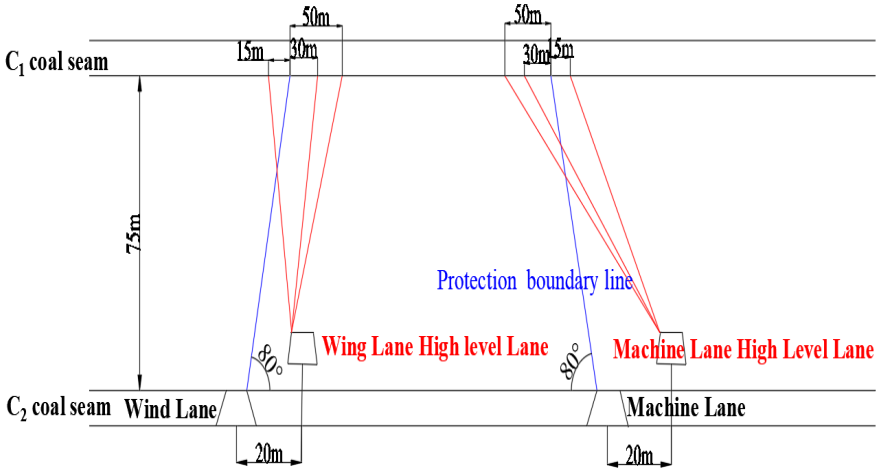

Fig. 9. Cross layer pressure relief drainage borehole layout section diagram

4.2. Analysis of pressure relief gas drainage effect and identification of pressure relief gas window period in C_1 coal seam

Under the mining influence of the C_2 coal seam, the distant protected C_1 coal seam underwent extensive depressurization and expansion deformation, leading to the formation of tensile-type horizontal fractures and their expansion and extension in the horizontal direction, thus forming lateral diffusion channels for gas permeation. This process significantly increased permeability, creating a time-space window that increased by several thousand times, which is the optimal "window period" for gas extraction. As mining progresses further, the protected layer enters the stress recovery zone, and the horizontal fractures in the coal seam gradually tend to close, with the fracture window also closing and disappearing. Therefore, the time-space stage where gas migration is active and horizontal fractures are developed constitutes the optimal "time window" for depressurization gas extraction.

During the field inspection of the depressurization borehole extraction window for the C_1 coal seam, it was observed that when the mining face advanced past the corresponding position in the C_2 coal seam by 50 meters, the depressurization area of the C_1 coal seam began to extract high concentrations of gas. The extraction concentration in most boreholes stabilized between 60% to 90% over a certain period. Random selections of the extraction holes 1-1#, 2-3#, 10-2#, and 15-1# were monitored for changes in extraction concentration, with detailed results presented in the following Fig. 10 and TABLE 4, used to determine the depressurization window period.

According to Fig. 10, the high concentration gas in the drainage hole of C1 coal seam continues to advance between 350 m and 375 m of the working face, and the time period from the working face advancing 50 m to 375 m is the effective window for depressurization gas extraction. The duration of the time window is inversely proportional to the advancement speed of the working face, identified as 85 to 100 days for the C_2 coal seam working face. Precisely capturing the gas extraction window for the C_1 coal seam plays a positive role in enhancing the efficiency of gas extraction from the C_1 coal seam, eliminating the risk of gas outbursts, and ensuring the safe and efficient retreat mining of the working face.

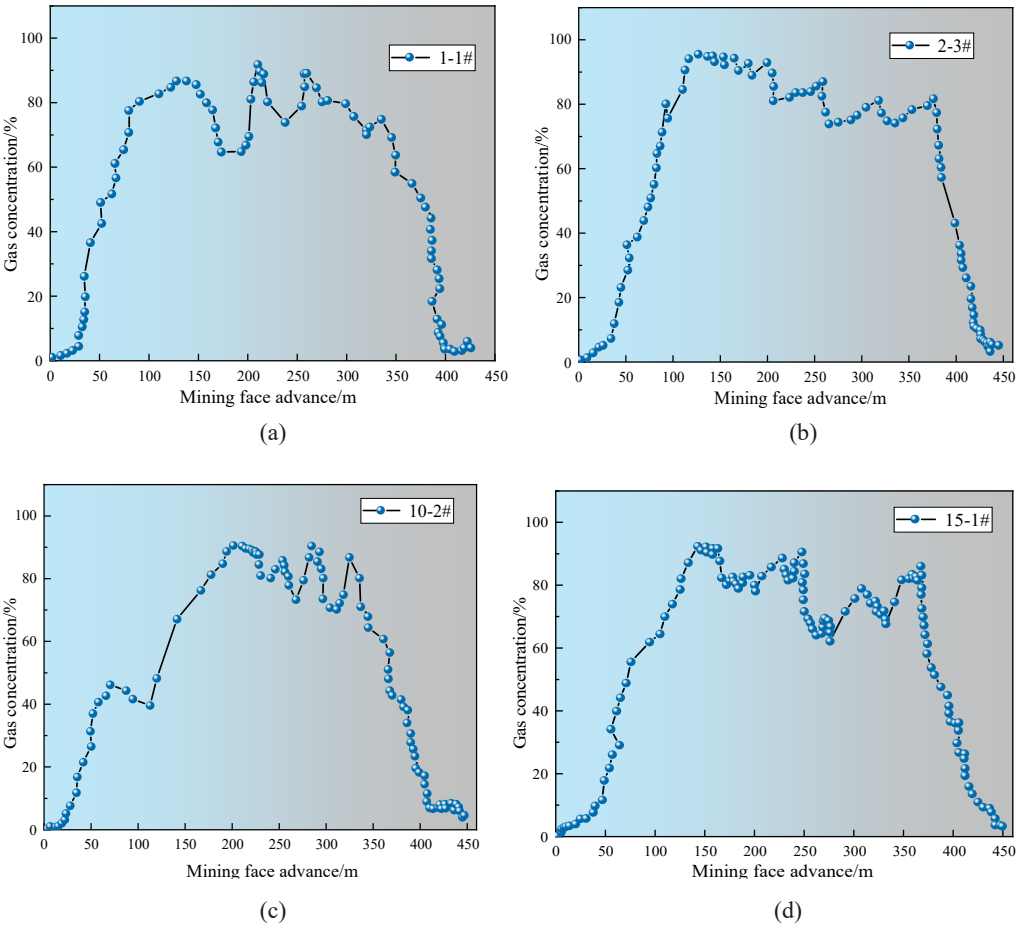

Fig. 10. Variation of gas extraction concentration in different boreholes
(a) Change in gas extraction concentration in hole 1-1#, (b)Changes in gas extraction concentrations in hole 2-3#, (c) Change in gas extraction concentration in hole 10-2#, (d) Change in gas extraction concentration in hole 15-1#

5. Conclusion

This study, **c**onducted during the mining period of a protective layer working face in a mine in Pingdingshan, involved experimental testing of the composition ratios of gas sources within the goaf to clarify the key tasks of gas control during the mining period of the protective layer. It also optimized the design of the depressurization gas extraction boreholes for the C_1 coal seam protected by the C_2 coal seam during the retreat mining period of the protective layer. The main conclusions of the study are as follows:

(1) There are significant differences in the stable carbon and hydrogen isotope values of desorbed gases from the main coal seams, mainly caused by differences in gas content and coal-forming environments. Additionally, as the burial depth increases, the carbon

isotope values of methane, ethane, hydrogen, and carbon dioxide gradually become heavier, indicating that the content of these gases increases with increasing depth.

(2) This study established a quantitative identification model for the volumetric ratio of mixed gases based on mass conservation, providing a solid theoretical basis for analyzing the proportions of gas sources in the goaf.

(3) The study found that the main source of gas in the goaf of the protective layer comes from the C_3 coal seam, accounting for 81%, while the C_2 coal seam accounts for only an average of 12%, and the C_1 coal seam for merely 7%. This indicates that vertical fractures did not develop effectively to the C_1 coal seam during the mining of the C_2 coal seam, preventing or minimally allowing depressurization gas to enter the goaf. This phenomenon causes the gas content in the C_1 coal seam to remain unchanged, posing a safety hazard for gas discharge from the C_1 coal seam.

(4) The study determined the optimal window period for gas extraction from the C_1 coal seam, which is when the C_2 coal seam working face advances from 50m to 375m, corresponding to 85 to 100 days. Gas extraction should be carried out during this optimal period when the gas seepage channels are forming, to eliminate the gas hazards in the C_1 coal seam.

Acknowledgement

This study was funded by a grant from the National Natural Science Foundation of China (Grant number: 51974239).

References

[1] L. Yuan, Strategic thinking of simultaneous exploitation of coal and gas in deep mining [J]. J. China Coal Soc. **41** (01), 1-6 (2016). DOI: https://doi.org/10.13225/j.cnki.jccs.2015.9027

[2] G. Qiao, Z. Liu, Y. Zhang, C. Yi, K. Gao, S. Fu, Y. Zhao, Theoretical analysis and engineering application of controllable shock wave technology for enhancing coalbed methane in soft and low-permeability coal seams [J]. Int. J. Coal Sci. Technol. **11** (25), 123-142 (2024). DOI: https://doi.org/10.1007/s40789-024-00673-1

[3] Y. Fu, Y. Wu, J. Li, P. Zhou, Z. Sun, J. He, Mechanical properties and energy evolutions of burst-prone coal samples with holes and fillings [J]. Int. J. Coal Sci. Technol. **11** (40), (2024). DOI: https://doi.org/10.1007/s40789-024-00675-z

[4] Q. Hao, A. Cao, C. Wang, Z. Tang, J. Liu, Numerical investigation on damage effect of deep hole pre-cracking roof rock and controlling rockburst [J]. Int. J. Coal Sci. Technol. **12** (1), (2025). DOI: https://doi.org/10.1007/s40789-025-00791-4

[5] W. Zhou, L. Yuan, G.L. Zhang, H.L. Du, S. Xue, G.H. He, Y.C. Han, A new method for determining the individual sources of goaf gas emissions:A case study in Sihe Coal Mine [J]. J. China Coal Soc. **43** (4), 1016-1023 (2018). DOI: https://doi.org/10.13225/j.cnki.jccs.2017.1136

[6] J.H. Shen, Y. Shi, B.Q. Lin, T. Liu, Y. Shen, T. Liu, X.L. Zhang, W. Yang, Study on the influence law of gangue filling structure on the gas emission in adjacent coal seams. J. Clean. Prod. **455**, 142339 (2024). DOI: https://doi.org/10.1016/j.jclepro.2024.142339

[7] Z.Q. Lan, G.S. Zhang, Numerical simulation of gas concen-tration field in multi-source and multi-congruence goaf [J]. J. China Coal Soc. **32** (4), 396-401 (2007). DOI: https://doi.org/10.3321/j.issn:0253-9993.2007.04.013

[8] W. Zhao, H. Dong, J. Ren, Y. Yuan, K. Wang, F. Wang, A software for calculating coal mine gas emission quantity based on the different-source forecast method [J]. Int. J. Coal Sci. Technol. **11** (51), (2024). DOI: https://doi.org/10.1007/s40789-024-00703-y

[9] M.G. Xu, H. F. Lin, H. Y. Pan, Numerical study of gas migra-tion in mechanized mining gob [J]. J. Hunan Univ. Sci. Technol. Nat. Sci. Ed. **25** (2), 6-9 (2010). DOI: https://doi.org/10.3969/j.issn.1672-9102.2010.02.002

[10] P. Li, Analysis of gas source in 1209 working face of a mine in SHANXI [J]. Inner. Mongolia Coal Eco. **21**, 45-46 (2018). DOI: https://doi.org/10.3969/j.issn.1008-0155.2018.21.023

[11] F.S. Mei, Pan Yidong Coal Mine of High Gas Coal Seam Coal Face Gas Source and Gas Governance Research [D]. Anhui Uni. Sci. Technol. (2014). DOI: https://doi.org/10.7666/d.Y2696871

[12] X.M. Li, F.Y. Sang, L.L. Sun, C.A. Du, Y.W. Hu, G. Wang, Assessment Methodand Application of Gas Resources in Abandoned Mine [J]. Min. Res. Dev. **39** (4), 101-104 (2019). DOI: CNKI:SUN:KYYK.0.2019-04-022

[13] Q.T. Hu, Y.P. Liang, J.Z. Liu, CFD simulation of goaf gas flow patterns [J]. J. China Coal Soc. **32** (7), 719-724 (2007). DOI: https://doi.org/10.3321/j.issn:0253-9993.2007.07.010

[14] J. Aditya, S. Claire, J.B. Jurgen, F.B. Gregory E., Computational Fluid Dynamics Modeling of a Methane Gas Explosion in a Full-Scale, Underground Longwall Coal Mine [J]. Mining Metall. Explor. **39** (3), 897-916 (2022). DOI: https://doi.org/10.1007/S42461-022-00587-Z

[15] C. Cheng, X.Y. Cheng, H. Gao, W.P. Yue, C. Liu, Prediction of Gas Emissions in the Working Face Based on the Desorption Effects of Granular Coal: A Case Study. Sustainability-Basel **14** (18), 11353-11353 (2022). DOI: https://doi.org/10.3390/su141811353

[16] S.D.Wang, Z. Qing, L.J. Yi, J.Z. Qian, Seepage Characteristics Study of Single Rough Fracture Based on Numerical Simulation. Appl. Sci. **12** (14), 7328-7328 (2022). DOI: https://doi.org/10.3390/app12147328

[17] Z.Y. Qin, L. Yuan, H. Guo, Q.D. Qu, Investigation of longwall goaf gas flows and borehole drainage performance by CFD simulation [J]. Int. J. Coal Geol. **151-152**, 51-63 (2015). DOI: https://doi.org/10.1016/j.coal.2015.08.007

[18] G.Y. Si, J.Q. Shi, S. Durucan, A. Korre, J. Lazar, S. Jamnikar, S. Zavek, Monitoring and modelling of gas dynamics in multi-level longwall top coal carving of ultra-thick coal seams, part II: Numerical modelling-Science Direct [J]. Int. J. Coal Geol. **144-145**, 58-70 (2015). DOI: https://doi.org/10.1016/j.coal.2015.04.009

[19] Z.F. Wang, W. Wu, Analysis on Major Borehole Sealing Methods of Mine Gas Drainage Boreholes [J]. Coal Sci. Technol. **42** (6), 31-34 (2014). DOI: https://doi.org/10.13199/j.cnki.cst.2014.06.006

[20] T.X. Wen, X. Sun, X.B. Kong, H.B. Tian, Research on prediction of gas emission quantity with sub sources basing on PSOBP-AdaBoost [J]. China Saf. Sci. J **26** (5), 94-98(2016). DOI: https://doi.org/10.16265/j.cnki.issn1003-3033.2016.05.017

[21] C.R. Wei, Y.X. Li, J.H. Sun, H.W. Mi, J. Li, Gas emission rate prediction in coal mine by grey and separated resources prediction method [J]. J. Min. Saf. Eng. **30** (4), 628-632 (2013).

[22] Y.X. Chai, W. Zhou, Quantitative Analysis Method of Gas Source in the First Mining Face of Zhuji Coal Mine Based on Carbon Isotope [J]. Saf. Coal Mines **50** (6), 176-180 (2019). DOI: CNKI:SUN:MKAQ.0.2019-06-044

[23] Y. Wang, Analysis of Isotope Gas Characteristics and Research and Application of Measurement Technology for Extraction and Separation of Gas Sources [J]. Sci. Technol. Inno. **12**, 54-55 (2020). DOI: CNKI:SUN:HLKX.0.2020-12-031

[24] Q.F. Liao, Analysis on Upper Corner Gas Source in Huangling No. 2 Coal Mine. Shanxi Cok. Coal Min. Technol. **43** (6), 43-45 (2019). DOI: https://doi.org/10.3969/j.issn.1672-0652.2019.06.013

[25] Z.Q. Wan, Study on the application and occurrence characteristics of trace elements in Two Huai coal mine [D]. Univ. Sci. Technol. China (2015).

[26] L.C. Zhu, J.X. Ma, Q.X. Song, W. Zhou, Application Study on Source Separation Predition of Gas in Xieqiao Mine [J]. Min. Const. Technol. **41** (04), 25-27 (2020). DOI: https://doi.org/10.19458/j.cnki.cn11-2456/td.2020.04.006

[27] W. Zhou, Study on the sources of gas emissions in coal mining based on stable caxbon and hydrogen isotopes and multi-source linear algorithm [D]. Anhui Univ. Sci. Technol. (2021). DOI: https://doi.org/10.26918/d.cnki.ghngc.2021.000012

[28] W. Zhou, S. Xue, Y. C. Han, C. Zheng, Application of stable carbon and hydrogen isotope technology in the determination of gas sources from limestone layers at Shuangliu mine, China [J]. J. Geophys. Eng. **18** (2), 282-290 (2021). DOI: https://doi.org/10.1093/jge/gxab013

[29] M. Schoell, Genetic characterization of natural gases [J]. Aapg. Bull. **67**, 2225-2238 (1983).

[30] X.Z. Gao, Volume Evaluation of the Gas Mixed With other Gases Using Carbon Isotopis Compositions [J]. Acta Sedimentol. Sin. **2**, 63-65 (1997). DOI: CNKI:SUN:CJXB.0.1997-02-012